Journal of Engineering Mathematics **38:** 77–90, 2000.

Restabilization in structures susceptible to localized buckling: an approximate method for the extended post-buckling regime

M. KHURRAM WADEE[1] and ANDREW P. BASSOM[2]
[1]*School of Engineering and Computer Science, University of Exeter, North Park Road, Exeter, Devon EX4 4QF, U.K.; e-mail: m.k.wadee@ex.ac.uk*
[2]*School of Mathematical Sciences, University of Exeter, North Park Road, Exeter, Devon EX4 4QE, U.K. Also with: New College, University of New South Wales, Sydney 2052, Australia; e-mail: a.p.bassom@ex.ac.uk*

Received 28 December 1998; accepted in revised form 18 June 1999

Abstract. Localized buckling in structures has been extensively studied in the context of simple nonlinear models which capture the essence of the phenomenon near the lowest critical load. In this study we apply a non-periodic Rayleigh–Ritz procedure to track localizations into the far post-buckling regime where the structure regains stability after the initial destabilization. The results are compared against independent numerical solutions and good agreement is found.

Key words: dynamical systems, double-scale perturbation, non-periodic Rayleigh–Ritz analysis, homoclinic and heteroclinic orbits, structural localization.

1. Introduction

Loss of elastic stability has been studied with much interest over the past few decades, as it has accounted for many failures of structures during construction and service. A fundamental understanding of buckling phenomena under *conservative* loading has been developed primarily through the use of the concepts of total potential energy and Hamilton's principle [1, pp. 16–19]. Buckling is a manifestation of a bifurcation phenomenon with a fundamental solution losing stability and being replaced by some other pattern: the bifurcation can be either super- or sub-critical, depending on the precise form of the nonlinearity.

Our concern will be with long one-dimensional structures which admit a zero or trivial fundamental state. For such simple cases early analyses concentrated almost exclusively on a deflection profile, where the buckling occurs in a distributed manner along the structure. This is the case of a post-buckling response, which is lateral deflection of the structure *periodic* in the axial coordinate [2, pp. 26–45]. When buckling is characterized by a stable post-buckling path, (*i.e.* the structural system experiences a super-critical bifurcation), then periodicity of the deflected profile of the structure is a reasonable assumption. However, if the structural system suffers a sub-critical bifurcation, the deflection tends not to be periodic but, rather, is limited to a small region of the structure. We define this as localization of buckle patterns and note that the solution dies off exponentially to zero either side of the large-deflection region, [3]. Asymptotic [4] and numerical [5] techniques have been developed which can find such solutions – at least in the case where the secondary path falls off monotonically from the critical state. However, in practice a structure often restabilizes and so the assumption of a simple nonlinearity which causes paths simply to fall and never to rise is inadequate for

studying more realistic systems. Where nonlinearity arises out of the large-deflection (elastica) geometry, some similar qualitative results are found [6].

Much progress has been made in the knowledge of localized buckling properties largely through the consideration of simplified model structures [7]. For instance, it is remarkable that the analysis of the one-dimensional model of a linear strut resting on a nonlinear foundation has had such a bearing on our understanding of the behaviour of much more complicated systems such as the axially-compressed cylindrical shell [8]. In the current study we wish to explore techniques for analysing a more realistic assumption for the behaviour of the nonlinearity of the strut system and, in particular, our desire is to look at a problem in which the foundation restabilizes after the initial instability. Work of a general nature on such a system has been reported by Woods and Champneys [9] who found that the post-buckling of the strut on a restabilizing foundation is characterized by a series of falling and rising paths as the deflection goes from being thoroughly localized to periodic.

For structures which localize and then restabilize the deflection eventually becomes periodic in the axial coordinate, but this does not occur until far into the post-buckling regime of the system. Past experience suggests that a periodic Rayleigh–Ritz analysis suffices to find the load at which the transition occurs between the localized and periodic states (for example see the results in [10, pp. 174–185]. It has been reasoned that the transfer from localized to periodic buckling occurs according to the classical Maxwell criterion for the change of a system from one equilibrium state to another. This hypothesis has recently been given a firm underpinning and the behaviour has been reported for other structural systems as well [11].

Our aim here is to investigate the accuracy of an approximation technique further into the post-buckling regime than has previously been reported. Our results show that, starting with an approximation to the primary localized solution, we can track post-buckling solutions and we continue the analysis beyond the point where the path restabilizes and a second loss of stability, through the occurrence of a fold catastrophe, is incipient. Woods and Champneys [9] have tracked the solution using a numerical boundary-value problem solver and we validate our modal results using the same software.

The work reported here begins with an introduction to the strut model to be studied starting with the total potential-energy functional and the governing differential equation. An analysis of the linearized form of this equation reveals the location of the critical point at which the trivial solution is replaced by a buckled response. At criticality, the linear response suggests a distributed form of solution is feasible, but under the right circumstances the chosen nonlinearities actually give rise to solutions which are localized to a small region of the structure. Section 3 outlines a double-scale perturbation to find the form of solution emerging from the critical point. The analysis predicts that localized solutions can not exist for all forms of nonlinearity. Although such asymptotic solutions have been shown to be good near the point of expansion, severe shortcomings have also been identified and some of these are highlighted. Section 4 shows the way in which the above asymptotic solutions can be used as a basis for performing a Rayleigh–Ritz type of analysis which again begins with the energy functional from which approximate equilibrium equations are derived. The solutions of these equations are compared with direct numerical integrations of the differential equation using an established piece of freely-available software – the comparisons are very good for the range of post-buckling under study. We finish by drawing some conclusions in Section 5.

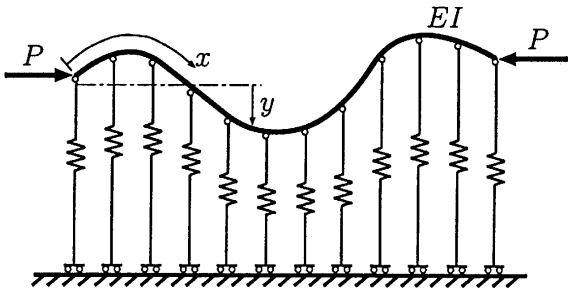

Figure 1. An elastic strut resting on an elastic foundation acted on by a compressive axial load.

2. Basic analysis

The structure to be studied is shown in Figure 1 in which x denotes the axial coordinate and y measures vertical deflection. An infinitely long strut, with a linear bending stiffness EI, rests on a nonlinear elastic foundation which provides a resistive vertical force F per unit length (see [2]). The structure is loaded by a compressive axial force P which maintains its direction and magnitude during any displacement: however this loading can be varied parametrically.

2.1. THE NONLINEARITIES

To ensure that the structural system undergoes a sub-critical bifurcation, when localized buckling is usually favoured over its periodic counterpart, the nonlinearity which dominates in this region must have a negative coefficient. Higher-order positive terms are then required to cause the system to restabilize. In order to model these various features we choose to capture the restabilization phenomenon at the lowest possible orders so that in addition to the linear term in the foundation force a negative quadratic term and a positive cubic term are included. Thus we take

$$F = ky - c_1 y^2 + c_2 y^3, \tag{1}$$

where the foundation constants k, c_1 and c_2 are all positive. Of course, this choice of nonlinearity is not unique, but does have the merit of exhibiting all the essential features required while maintaining some simplicity.

In order to find valid equilibrium states (and then subsequently to assess their stability) we must consider the total potential energy of our structural system. This has two major components. First, there is strain energy U which is the energy stored in deforming the structure. Second, there is the work done by the external load(s) P which for a conservative system can be denoted by $P\mathcal{E}$ where $\mathcal{E}$ is the distance moved by the load in its direction of action (for our one-dimensional system we call $\mathcal{E}$ end-shortening). Taken together, these two components of energy form the total potential energy of the system

$$V = U - P\mathcal{E} \tag{2}$$

which for the strut is

$$V = \int_{-\infty}^{\infty} (\tfrac{1}{2} EI\ddot{y}^2 - \tfrac{1}{2} P\dot{y}^2 + \tfrac{1}{2} ky^2 - \tfrac{1}{3} c_1 y^3 + \tfrac{1}{4} c_2 y^4)\, \mathrm{d}x, \tag{3}$$

where a dot denotes diffentiation with respect to x[3]. The various parts of (3) admit physical interpretations which can be motivated by considering a small element of the strut of length dx. The first three terms in the integrand come from the standard truncation of the Taylor-series expansions for the expressions for the bending energy stored in the element, the work done by the load P in moving from the undeflected to the deflected state of the element and the amount of energy stored in the foundation due to the linear stiffness k. The remaining two terms arise from the nonlinear parts of the foundation response [2].

Equilibrium states are defined as those at which V takes extreme values for arbitrary variations in V. The governing equation is found upon application of the calculus of variations to the expression for the first variation of V and is readily obtained as

$$EI\,\dddot{y} + P\ddot{y} + ky - c_1y^2 + c_2y^3 = 0. \tag{4}$$

In order to highlight the roles of the linear and nonlinear terms the above equation can be rescaled so that only the essential coefficients remain as free parameters. Henceforth, we will examine a dimensionless form of (4) by setting $EI = k = c_1 = 1$ [5] which yields the simplified form

$$\dddot{y} + P\ddot{y} + y - y^2 + c_2y^3 = 0. \tag{5}$$

Now the constant c_2 characterizes the degree of restabilization of the foundation.

2.2. Linear eigenvalue analysis

The loading on the structure is parametrized by P and we need to find the value at which the flat fundamental (unbuckled) state loses stability. It suffices to examine a linearized form of (5) and, for positive P, three regions with distinct behaviours are identified (Figure 2). For the range $P > P^C = 2$, the eigenvalues of (5) take four distinct imaginary values symmetrically spaced about the real axis. The deflection in this case is thus expected to be periodic in x. As P is reduced the pairs either side of the real axis coalesce and, subsequently, the system undergoes a Hamiltonian–Hopf bifurcation as the two pairs split symmetrically into the four quadrants of the complex plane with the forms $\pm\alpha \pm i\omega$ where

$$\alpha = \sqrt{\frac{1}{2} - \frac{P}{4}}, \qquad \omega = \sqrt{\frac{1}{2} + \frac{P}{4}}. \tag{6}$$

At the critical point the quadratic nonlinearity will dominate over the cubic term and the initial path is found to fall from P^C [2]. Thus we expect the region $P < P^C$ to be of importance for our post-buckling study and here the linearized behaviour is a sinusoidal wave bound by an exponentially growing or decaying envelope. Past experience [4] indicates that the nonlinearity in the system is capable of forming a connection between growing and decaying solutions leading to a strut profile which is localized in x. In dynamical systems terminology, the system is Hamiltonian with an associated spatial analogue of potential energy and kinetic energy and localized profiles are homoclinic to the flat state [5].

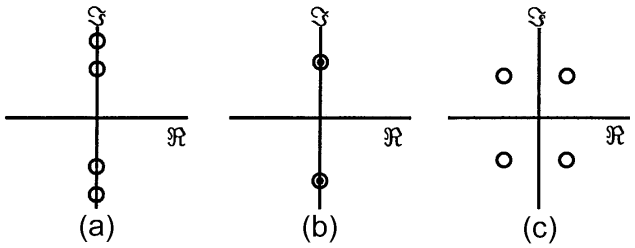

Figure 2. Eigenvalues of the linearized form of (5) for (a) $P > P^C = 2$, (b) $P = P^C$ and (c) $P < P^C$.

3. Double-scale perturbation analysis results

In the vicinity of P^C a double-scale perturbation analysis reveals the behaviour of the emergent primary solutions. To this end we define a perturbation parameter ε which measures evolution from the critical state such that

$$P = P^C - \varepsilon^2 + \cdots. \tag{7}$$

In previous analyses (see [3], for example), this expansion has been truncated after the second term but we may wish to include the extra terms because the restabilization may impose an effect on P such that other terms are involved. However, to the level shown below, no such effect has been found. Also, because the behaviour at $P = P^C$ is expected to be sinusoidal a solution in this vicinity can be assumed to evolve smoothly from there. The amplitude of the solutions may vary on a shower scale than the period of the deflection at $P = P^C$ and so we define a slow space scale such that

$$X = \varepsilon x. \tag{8}$$

By expressing y as

$$y = \sum_{i=0}^{\infty} \{A_i(X) \cos i(\omega x + \phi_0) + B_i(X) \sin i(\omega x + \phi_0)\}, \tag{9}$$

where A_i and B_i are slowly varying amplitudes and ϕ_0 is a phase angle, we may transform the governing equation (5) into a partial differential equation [4]. The slow-space analysis, which is the one we are concerned with here, completely decouples the fast variation from the slow one [5] and, in particular, suggests that the phase ϕ_0 is arbitrary. However, a more advanced analysis based upon the ideas of exponential asymptotics reveals that for primary localization ϕ_0 is not free, but rather is restricted to the discrete values $\phi_0 = 0, \pi$ [12]. This reinforces the importance of the symmetric section which means that all primary solutions to this system must be even functions about their own centres [4].

If each amplitude is also expressed as a series in ε

$$A_i(X) = \sum_{j=1}^{\infty} \varepsilon^j A_i^{(j)}(X), \qquad B_i(X) = \sum_{j=1}^{\infty} \varepsilon^j B_i^{(j)}(X) \tag{10}$$

and progressively higher-order coefficients of ε are extracted, we derive a set of equations which reveal the behaviour of the amplitudes in the formal expansions of each A_i and B_i. The

somewhat labour-intensive details of this procedure are relegated to Appendix A from which it is seen that the first equation giving non-trivial information concerning the amplitude of the fundamental mode $A_1^{(1)}$ is

$$4\frac{\mathrm{d}^2 A_1^{(1)}}{\mathrm{d}X^2} - A_1^{(1)} + \left(\frac{19}{18} - \frac{3}{4}c_2\right) A_1^{(1)3} = 0. \tag{11}$$

For bounded localized solutions the coefficient of the cubic term must be positive which yields the condition

$$c_2 < \frac{38}{27}, \tag{12}$$

whereupon

$$A_1^{(1)} = 6\left(19 - \frac{27}{2}c_2\right)^{-1/2} \operatorname{sech}\left(\frac{X}{2}\right). \tag{13}$$

For larger values of c_2 the asymptotic theory predicts that localized solutions cannot exist and this result ties in precisely with the study of Woods and Champneys [9] who used a normal forms type of analysis for the restabilizing strut problem. Apart from this condition on c_2, Equation (11) is only expected to be valid very close to the critical point at $P = P^C$ and gives no idea as to how the system may evolve when ε is not small.

Like earlier attempts at approximating and tracking localized post-buckling solutions some way into that regime with a regular double-scale approach [3, 4] there is no indication of other types of behaviour that may be expected in post-buckling. Even if higher-order terms are calculated, nothing new is revealed about the existence of subsidiary localized solutions or the eventual effect of the restabilization. In addition to developing global proofs for the system [13], two ways to proceed have been proposed. One is to track the primary solutions using a Rayleigh–Ritz [5] technique. The other is to modify the relatively simple-minded double-scale asymptotics to incorporate beyond-all-orders terms and so find subsidiary localizations [14]. Here we shall pursue the former strategy as we are interested in the way that the stability of the initial localized profile changes.

The ability of the foundation to restabilize after the initial instability is characterized by the coefficient of the cubic term c_2 in (5). Different values of c_2 can give qualitatively different foundation responses as is demonstrated by Figure 3 which shows the form of the foundation force $F = y - y^2 + c_2 y^3$ for three values $c_2 \in [0{\cdot}24, 0{\cdot}4]$. Now (12) predicts that for all c_2 in this interval localization may occur but the plots in Figure 3 cover a variety of quite different responses. It may be argued that the case $c_2 = 0{\cdot}24$ is physically unrealistic because there is a range of positive deflection, y, for which the foundation does not resist deflection ($F > 0$) but in fact favours it ($F < 0$). On the other hand, this objective is equally valid of the quadratic foundation (*i.e.* $c_2 = 0$) studied by Hunt *et al.* [3] and by many subsequent researchers. When $c_2 = 0{\cdot}30$ Figure 3 proves that the foundation response is always resistive but the stiffness (gradient) of the foundation force is negative for a range of deflections. In contrast, for the last case shown ($c_2 = 0{\cdot}40$) the foundation merely loses some stiffness at some point but this quantity is always positive.

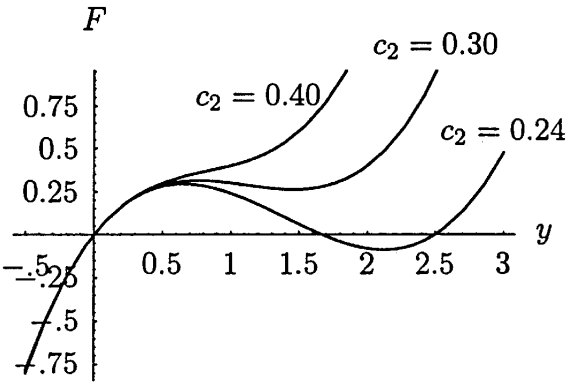

Figure 3. The variation of foundation force $F = y - y^2 + c_2 y^3$ against lateral deflection y for various values of the constant c_2.

4. Non-periodic Rayleigh–Ritz analysis

Irrespective of the size of c_2 in (5), the quadratic component dominates the nonlinear response in the vicinity of P^C so we would expect the same form of passive modes to appear as when F is simply given by $F = y - y^2$. Wadee *et al.* [5] performed an extended analysis of the equations for the quadratic nonlinearity problem and derived a system of equations using the double-scale approach. In Appendix B we derive the equivalent results for our restabilization problem which shows that the complete form of the solution emerging from the bifurcation point is

$$y = \varepsilon A_1^{(1)} \cos(\omega x + \phi_0) + \varepsilon^2 \{A_0^{(2)} + B_1^{(2)} \sin(\omega x + \phi_0) + A_2^{(2)} \cos 2(\omega x + \phi_0)\} + \mathcal{O}(\varepsilon^3). \tag{14}$$

Here $A_1^{(1)}$ is given by (13), $A_0^{(2)} = \frac{1}{2} A_1^{(1)2}$, $A_2^{(2)} = \frac{1}{18} A_1^{(1)2}$ (see (A3) and (A4)) and $B_1^{(2)}$ is as shown in Equation (B5) of Appendix B. This perturbation solution can only be expected to be accurate for reasonably small values of ε. Once P is appreciably less than $P^C (= 2)$ then, as we discussed earlier, one of the few methods by which analytical progress is possible is via a Rayleigh–Ritz approach.

Of course, of utmost importance for the successful implementation of a Rayleigh–Ritz procedure is a good choice for the initial trial function. The usual obstacle that one has to face is of dual but conflicting issues: on the other hand, if too simple a function is taken, then it is unlikely to be able to capture the details of the physics involved, but if it is too complicated, the resulting analysis may become very time-consuming if not totally impractical. To steer a path between these problems and guided by the results above, deflections were sought with the approximate form

$$y = A_1 \operatorname{sech} \alpha x \cos \omega x + A_0 \operatorname{sech}^2 \alpha x + A_2 \operatorname{sech}^2 \alpha x \cos 2\omega x + B_1 \operatorname{sech} \alpha x \tanh \alpha x \sin \omega x + C_1 \operatorname{sech}^3 \alpha x \cos \omega x + D_1 \operatorname{sech}^3 \alpha x \tanh \alpha x \sin \omega x. \tag{15}$$

The first three terms arise from the obvious generalization of the $O(\varepsilon^2)$ solution (14) with the phase $\phi_0 = 0$ so as to incorporate the formal exponential asymptotics result obtained by

[12] and $X/2$ in (14) is to be identified with αx. The remaining parts of (15) are motivated by the higher-order active solutions outlined in Appendix B, see (B4), (B5) and the subsequent comments concerning the forms of solutions $A_1^{(3)}$ and $B_1^{(4)}$. Last, it is important to emphasize that the unknown coefficients A_1, A_0, etc. in (15) should not be confused with the known functions in (14).

In the usual Rayleigh–Ritz procedure the coefficients within (15) are treated as generalized coordinates and the whole expression fed into the V function (3). The result is a complicated and lengthy expression which contains numerous integrals, an example of which is

$$I_{cnm} = \int_{-\infty}^{\infty} \operatorname{sech}^n \alpha x \cos m\omega x \, \mathrm{d}x. \tag{16}$$

We can program closed-form expressions for such integrals as Mathematica routines [15], using appropriate complex integrals around suitable contours and implementing Cauchy's residue theorem. The equilibrium is given by the solution to

$$\frac{\partial V}{\partial A_0} = 0, \qquad \frac{\partial V}{\partial A_1} = 0, \quad \text{etc.} \tag{17}$$

and is located by exporting exact expressions for the various partial derivatives into user-written *C* routines. The forms of (17) are far too involved to solve by direct means so use was made of Newton's algorithm [16, pp. 362–371].

An innovation introduced by Wadee *et al.* [5] was to treat the quantities α and ω (the shape factors in (15)) as generalized coordinates rather than being taken as prescribed according to (6). On the face of it, this action seems somewhat perverse, as y is not linear in these variables. Whereas for the quadratic nonlinearity there were some arguably minor improvements in the accuracy of solutions when this extra flexibility was introduced, this additional feature is vital for our current work. Now it is essential that the shape factors are *not* explicitly functions of load (as would be the case if we imposed (6) for instance). The restabilization component in our model means that solutions are very likely be multi-valued in P as they are tracked into the restabilized region and conventional Rayleigh–Ritz procedures would soon fail.

To check the validity of the Rayleigh–Ritz solutions we used the boundary-value solver AUTO97 [17] which incorporates special routines to continue homoclinic orbits. From a value of P near critical it is possible to follow the primary solution all the way to a point where the solution encounters a limit point. At this point the continuation in P clearly fails but is possible to extend the solutions by exchanging the continuation parameter. If the continuation is performed not on P, but rather on one of the generalized coordinates, it is possible to obtain further solutions in the vicinity of the limit point. Attention can then be swapped back to P and simple continuation in that parameter used again. Thus, with a little skulduggery we are able to track around folds with our modal approach. AUTO, on the other hand, is able to deal with folds and detect bifurcations quite satisfactorily.

A graph of the variation of amplitude $y(0)$ of the primary localized solution versus load is shown in Figure 4 for the three values of c_2 in Figure 3. We have followed the Rayleigh–Ritz solution from near critical around the first local minimum of load and up to and beyond the next local maximum and over this range the numerical and our approximate solutions

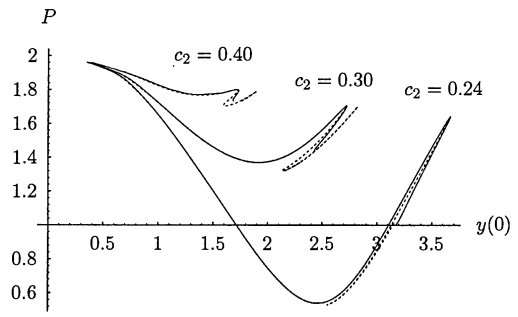

Figure 4. Variation of load against central amplitude of primary localization. Rayleigh–Ritz results are shown by solid lines and the AUTO results by dotted lines.

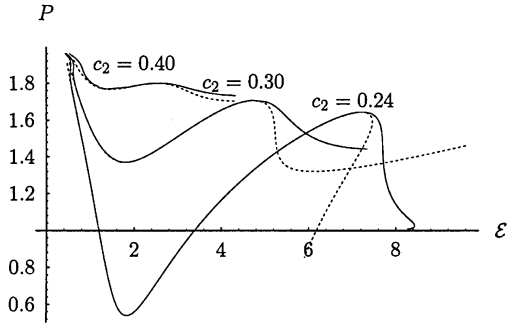

Figure 5. Variation of load against end-shortening $\boldsymbol{\varepsilon}$. Rayleigh–Ritz results are shown by solid lines and the AUTO results by dotted lines.

are virtually indistinguishable. It is only after this stage that the approximate and numerical solutions begin to diverge. The numerical results show that the dependence of the loading on the central amplitude $y(0)$ begins to oscillate wildly and it is unsurprising that the Rayleigh–Ritz procedure is unable to follow this given our fairly simple form of trial function (15).

Figure 5 shows the variation of load against end shortening $\boldsymbol{\varepsilon}$: a quantity that is easily calculated by extracting the appropriate expression from (3) [2]

$$\boldsymbol{\varepsilon} = \frac{1}{2}\int_{-\infty}^{\infty} \dot{y}^2 \, \mathrm{d}x. \tag{18}$$

In the Rayleigh–Ritz approach we used contour integration to find $\boldsymbol{\varepsilon}$ after substituting (15) in (18), while for the AUTO calculations we could find $\boldsymbol{\varepsilon}$ directly by introducing a dummy integral constraint.

The area under each curve in Figure 5 represents the work done in getting from the unloaded flat state to the particular point on the graph. Thus, this set of curves has physical significance and it is once again noteworthy that the modal solution appears identical to the numerical one up to the second limit point (first maximum) in the solution. Thereafter the two techniques yield diverging solutions although for the larger values of c_2 this divergence is not too severe. The other location where the numerical and Rayleigh–Ritz solutions show some differences is a small region in the vicinity of P^C. This anomaly was also found in the case of a softening quadratic foundation [5]. Unfortunately, we cannot offer any convincing explanation for this behaviour so close to P^C where we would expect a high degree of accuracy in both the perturbation results and the Rayleigh–Ritz solutions. However, in passing we note that in this limit $\alpha \to 0$ and so integrals of the type I_{cnm} (see (16)) with $m = 0$ become large compared with those for which $m \neq 0$. Recall that in (15) we motivated the various parts of the trial function by ensuring that we have counterparts of the passive modes up to $\mathcal{O}(\varepsilon^2)$ and of the active modes up to $\mathcal{O}(\varepsilon^4)$. When P is very close to $P^C (\varepsilon \ll 1)$, it is likely that we could achieve better variational results (with the same number of variables) by exchanging some of the higher order active parts of the solution for lower-order passive ones. However, as at such small values of ε very good results can be obtained directly from the perturbative scheme, a recasting of the variational formulation seems superfluous.

The accuracy of the modal results is evidenced by the precision of the match with the AUTO solutions for almost all of the post buckling region considered in Figures 4 and 5.

The agreement of the central amplitudes and overall end shortenings both give us a degree of confidence in the solutions, at least up to the first maxima. As further evidence as to the comparisons, Figure 6 shows the form of $y(x)$ at the second limit points of Figure 5 and near where the final breakdown of the Rayleigh–Ritz forms occur. Two of the c_2 values are taken and it is clear from Figures 6a and 6c that at the maximums of the end-shortening graphs the numerical and approximate solution functions are virtually identical. Notice that, as the breakdown points are approached, subsidiary humps in the solutions grow markedly compared with the central maximum (*cf.* Figure 6a with 6b and 6c with 6d). The agreements between the two solution techniques, while no longer indistinguishable, is still eminently satisfactory, although it is noted that the main discrepancy begins to show in the details of the secondary humps – the central portions of the solutions are still captured remarkably well. Moreover, as the solutions begin to show signs of becoming increasingly distributed in nature, it is not surprising that our Rayleigh–Ritz forms, which recall were motivated by the two-scale perturbation results for localized solutions, find it more-and-more difficult to reproduce the numerical findings.

5. Conclusions

A successful application of a non-periodic Rayleigh–Ritz procedure has been reported which is capable of finding accurate solutions an appreciable way into the post-buckling regime of a strut resting on an elastic foundation. The recent paper by Woods and Champneys [9] indicates that the solution accumulates more waves around the centre of localization and eventually become periodic with the formation of a heteroclinic orbit connecting the flat state with one with constant amplitude at a point where the spatial analogue of overall energy is equivalent.

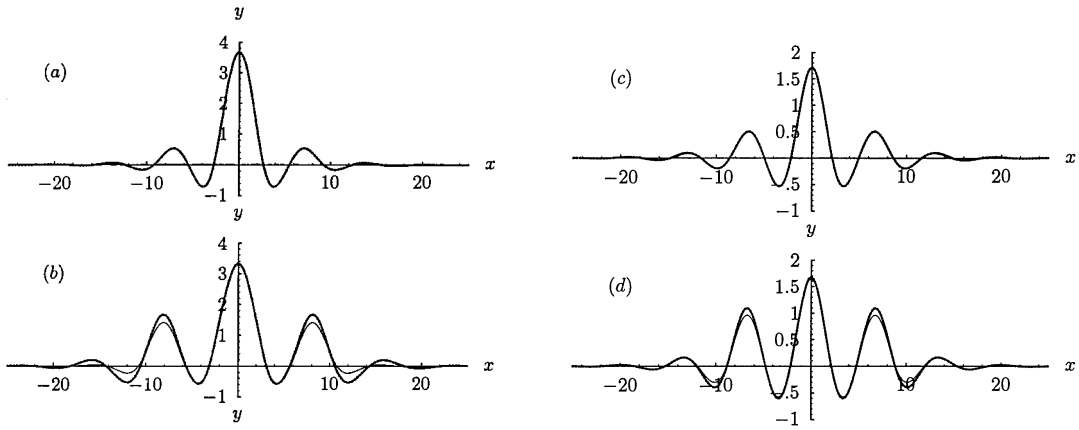

Figure 6. Localized deflection profiles for (5) with $c_2 = 0{\cdot}24$ (for (a) and (b)) and $c_2 = 0{\cdot}40$ ((c) and (d)). Graphs (a) and (c) are plotted at the location of the maximum of the respective load-end-shortening curve shown in Figure 5 and the numerical and Rayleigh–Ritz solutions are shown together but are indistinguishable. Plots (b) and (d) are shown near the point at which the Rayleigh–Ritz solutions break down ($P = 1{\cdot}20$ and $P = 1{\cdot}74$ respectively). The Rayleigh–Ritz solutions are plotted using the thick line and AUTO solutions by thin lines.

The double-scale equations give no inkling of the effect of a restabilizing term in the foundation response but merely predicts the monotonic growth of a sinusoidal solution with a slowly-varying amplitude. However, using this very form of solution as a basis for a non-periodic Rayleigh–Ritz procedure, we have been able to track the sub-critical behaviour of the

system extremely closely to that obtained by an independent numerical method at least up to the point where the structure once again loses stability. As expected a loss in the accuracy of the solution occurs soon after this stage because, as the solution becomes more disparate with an increasing number of humps being formed either side of the centre of solution, the choice of the modal form (15) for y seems then to be inappropriate. In the limit of full periodicity, our solution may once again become accurate with $\alpha = 0$. However, in that case it would seem much more sensible to perform a truly periodic analysis in preference to the approach adopted here.

We would contend that our non-periodic Rayleigh–Ritz procedure has shown itself to be a useful engineering tool for investigating the properties of a structural system with complicated stabilization characterisitics. Perturbation analysis can be used effectively for loadings P close to P^C and harmonic Rayleigh–Ritz methods are appropriate in the limit of periodicity. Our method outlined here attempts to a form a bridge between these extremes. With such a simple trial function as we have here, it is unreasonable to expect our approximations to be good for the whole domain between localized and periodic forms but it is pleasing just how far into the post-buckling regime our results remain accurate. Nothing we have done entitles us to expect such good results, but we have demonstrated that it is possible to track up to and beyond the second limit point without noticeable error. This raises the exciting possibility that a non-periodic Rayleigh–Ritz procedure is a good modal technique for investigating homoclinic and perhaps other types of behaviour. We include here the study of perturbed systems which can admit soliton-like solutions: obviously there is a wide class of problems of this type within structural mechanics involving more complicated geometries like elastica and shells. In addition, there is the possibility of extending our ideas into other aspects of solid and fluid mechanics where ‘near-soliton’-like behaviour can be observed. Clearly this aspect requires further studies and it would be surprising if progress can not be made. Given the impressive accuracy we have already achieved, a more refined selection of the trial function (15) could be expected to bear fruit.

To conclude, here we have been particularly interested in the initiation of the process of restabilization and how the solution which emerges at the bifurcation point evolves. To the best of our knowledge this is the first example of a non-periodic Rayleigh–Ritz procedure used in an engineering application where sensitive tracking around folds has been required. For the reasons outlined earlier, it is imperative that this modified form of Rayleigh–Ritz is implemented for a standard harmonic type of analysis would be quite unable to cope with the swaps in the nature of the stabilization of the strut. It is gratifying how the Rayleigh–Ritz method has given a very accurate description of the beginnings of the restabilization and it holds the promise of being extended usefully to other more complicated problems. We hope to be able to proceed further with the current technique, but we also foresee the need to incorporate a more sophisticated analysis which predicts the accumulation of many large-amplitude ‘humps’ around the primary orbit in the limit of periodicity.

Acknowledgements

We are very grateful to the referees for their comments which led to an improved account of our work. This study was completed while the second author was at the School of Mathematics, University of New South Wales. Thanks are due to both the staff of the School (especially Peter Blennerhassett) and to the staff and students of New College, UNSW for their hospitality.

Appendix A: Derivation of the double-scale equations

The analysis which leads to Equation (11) is an adaptation of that given by Wadee *et al.* [5]. We present the important elements here although the interested reader is directed to [5] for a full exposition of the methods involved.

We take the governing differential equation (5) and, noting the relationship between X and x in (8), substitute $P = P^C - \varepsilon^2 = 2 - \varepsilon^2$ to give

$$\varepsilon^4 y_{XXXX} + 4\varepsilon^3 y_{XXXx} + 6\varepsilon^2 y_{XXxx} + 4\varepsilon y_{Xxxx} + y_{xxxx} + (2-\varepsilon^2)(\varepsilon^2 y_{XX} + 2\varepsilon y_{Xx} + y_{xx}) + y - y^2 + c_2 y^3 = 0, \tag{A1}$$

where a subscripted letter denotes partial differentiation with respect to that variable. From (6) we see that the wavenumber, ω, can also be expressed as a power series in ε

$$\omega = 1 - \frac{\varepsilon^2}{8} + \cdots. \tag{A2}$$

After inserting the forms of solution (9), together with the series expansions (10) for $A_i(X)$ and $B_i(X)$, we obtain transcendental equations for the unknowns. Of course, the nonlinearity present ensures that interaction occurs between modes.

For a uniformly valid solution we require that the expressions are satisfied at progressively higher powers of ε. If we assume that the modes associated with the critical load $P^C = 2$ are A_1 and B_1 then all other modes can be shown to be at least locally quadratic in these active modes [5] (this is known as elimination of passive coordinates or Lyapunov–Schmidt reduction [2]). The lowest order at which expressions arise is $\mathcal{O}(\varepsilon^2)$ and at this stage equations for modes $A_0^{(2)}$, $A_2^{(2)}$ and $B_2^{(2)}$ are obtained. For example, $A_0^{(2)}$ is defined in terms of $A_1^{(1)}$ and $B_1^{(1)}$ by

$$A_0^{(2)} = \tfrac{1}{2}(A_1^{(1)2} + B_1^{(1)2}), \tag{A3}$$

while the other two equations at this order yield

$$A_2^{(2)} = \tfrac{1}{18}(A_1^{(1)2} - B_1^{(1)2}) \tag{A4}$$

and

$$B_2^{(2)} = \tfrac{1}{9} A_1^{(1)} B_1^{(1)}. \tag{A5}$$

At the next order, $\mathcal{O}(\varepsilon^3)$, we get the first appearance of equations which give non-trivial information about the active modes at order ε (*i.e.* $A_1^{(1)}$ and $B_1^{(1)}$):

$$4\frac{\mathrm{d}^2 A_1^{(1)}}{\mathrm{d}X^2} - A_1^{(1)} + 2A_0^{(2)} A_1^{(1)} + A_1^{(1)} A_2^{(2)} + B_1^{(1)} B_2^{(2)} - \tfrac{3}{4} c_2 A_1^{(1)} \left(A_1^{(1)2} + B_1^{(1)2} \right) = 0, \tag{A6}$$

$$4\frac{\mathrm{d}^2 B_1^{(1)}}{\mathrm{d}X^2} - B_1^{(1)} + 2A_0^{(2)} B_1^{(1)} - A_2^{(2)} B_1^{(1)} + A_1^{(1)} B_2^{(2)} - \tfrac{3}{4} c_2 B_1^{(1)} \left(A_1^{(1)2} + B_1^{(1)2} \right) = 0. \tag{A7}$$

Symmetry arguments lead to the conclusion that we can safely put $B_1^{(1)} = 0$ without loss of generality. Substituting expressions (A3)–(A5) in (A6) leads directly to Equation (11) and hence solution (13).

Appendix B: Remarks concerning higher order terms

Given the perturbative strategy outlined above, it is (theoretically) straightforward to pursue the calculations to as many orders as we please. To illustrate how this develops, here we mention the results of the $\mathcal{O}(\varepsilon^4)$ problem. Of course, the passive components of the calculation lead to $\mathcal{O}(\varepsilon^4)$ terms in (9), but it is at this point we uncover the details of the $\mathcal{O}(\varepsilon^2)$ active parts. Indeed, the comparison of $\sin(\omega x + \phi_0)$ and $\cos(\omega x + \phi_0)$ terms in (A1) show that

$$\mathcal{L}(A_1^{(2)}) = 0 \tag{B1}$$

and

$$\mathcal{L}(B_1^{(2)}) = \tfrac{8}{27} A_1^{(1)2} \frac{\mathrm{d}A_1^{(1)}}{\mathrm{d}X} + \frac{\mathrm{d}A_1^{(1)}}{\mathrm{d}X} - 4\frac{\mathrm{d}^3 A_1^{(1)}}{\mathrm{d}X^3}, \tag{B2}$$

where we have denoted

$$\mathcal{L}(\cdot) := 4\frac{\mathrm{d}^2(\cdot)}{\mathrm{d}X^2} + \left[\left(\frac{19}{18} - \frac{3}{2}c_2\right) A_1^{(1)2} - 1\right](\cdot). \tag{B3}$$

The bounded solutions of this pair of equations are

$$A_1^{(2)} = 0 \tag{B4}$$

and

$$B_1^{(2)} = \tfrac{1}{4}(19 - \tfrac{27}{2}c_2)^{-3/2}[374 - 243c_2]\,\mathrm{sech}\left(\frac{X}{2}\right)\tanh\left(\frac{X}{2}\right). \tag{B5}$$

The calculation of higher order active modes reveals an interesting structure. For instance

$$\mathcal{L}(A_1^{(3)}) = \mathrm{RHS}, \qquad \mathcal{L}(B_1^{(3)}) = 0, \tag{B6}$$

so that $B_1^{(3)} = 0$ and the form of RHS is such that $A_1^{(3)}$ comprises two parts: one proportional to $\mathrm{sech}^3(X/2)$ and the other proportional to $\mathrm{sech}(X/2)$. In other words, $A_1^{(3)}$ is a multiple of $A_1^{(1)}$ plus a multiple of $A_1^{(1)}\,\mathrm{sech}^2(X/2)$. This pattern continues to yet further orders, so $B_1^{(4)}$ is partly proportional to $B_1^{(2)}$, see (B5), together with a multiple of $\mathrm{sech}^3(X/2)\tanh(X/2)$. The details of the multiplying constants are immaterial for the Rayleigh–Ritz method but it is of interest that the solutions for the active modes are all combinations of terms like $\mathrm{sech}^m(X/2)\tanh^n(X/2)$ where $m \geqslant 1$ and $n \geqslant 0$ and these functions decay exponentially as $|X| \to \infty$.

References

1. C. Fox, *An Introduction to the Calculus of Variations*. London: Oxford University Press (1963) 271pp.
2. J. M. T. Thompson and G. W. Hunt, *A General Theory of Elastic Stability*. London: Wiley (1987) 322pp.
3. G. W. Hunt, H. M. Bolt and J. M. T. Thompson, Structural localization phenomena and the dynamical phase-space analogy. *Proc. R. Soc. London A* 425 (1989) 245–267.
4. G. W. Hunt and M. K. Wadee, Comparative lagrangian formulations for localized buckling. *Proc. R. Soc. London A* 434 (1991) 485–502.
5. M. K. Wadee, G. W. Hunt and A. I. M. Whiting, Asymptotic and Rayleigh–Ritz routes to localized buckling solutions in an elastic instability problem. *Proc. R. Soc. London A* 453 (1997) 2085–2107.
6. G. W. Hunt, M. K. Wadee and N. Shiacolas, Localized elasticæ for the strut on the linear foundation. *Trans. ASME J. Appl. Mech.* 60 (1993) 1033–1038.
7. M. K. Wadee, The elastic strut on an elastic foundation: A model localized buckling problem. In: A. R. Champneys, G. W. Hunt and J. M. T. Thompson (eds.), *Localization and Solitary Waves in Solid Mechanics*. Singapore World Scientific (1999). To appear.
8. G. J. Lord, A. R. Champneys and G. W. Hunt, Computation of localized post buckling in long axially compressed cylindrical shells. *Phil. Trans. R. Soc. London A* 355 (1997) 2137–2150.
9. P. D. Woods and A. R. Champneys, Heteroclinic tangles and homoclinic snaking in the unfolding of a degenerate reversible Hamiltonian Hopf bifurcation. *Physica D* (1999) Volume 129, pp. 147–170.
10. M. K. Wadee, *Elements of a Langrangian Theory of Localized Buckling*. PhD thesis: Imperial College of Science, Technology and Medicine, London (1993) 245pp.
11. G. W. Hunt, M. A. Peletier, A. R. Champneys, P. D. Woods, M. A. Wadee, C. J. Budd and G. J. Lord, Cellular buckling in long structures. *Nonlinear Dynamics* (1999) to appear.
12. T.-S. Yang and T. R. Akylas, On asymmetric gravity–capillary solitary waves. *J. Fluid Mech.* 330 (1997) 215–232.
13. A. R. Champneys and J. F. Toland, Bifurcation of a plethora of multi-modal homoclinic orbits for Hamiltonian systems. *Nonlinearity* 6 (1993) 665–721.
14. M. K. Wadee and A. P. Bassom, Effects of exponentially small terms in the perturbation approach to localized buckling. *Proc. R. Soc. London A* (1999). Volume 455, pp. 2351–2370.
15. Wolfram Research Inc., MATHEMATICA: *A System for doing Mathematics by Computer*. Champaign, Illinois: Wolfram Research, Inc. (1995) 749pp.
16. W. H. Press, B. P. Flannery, S. A. Teukolsky and W. T. Vetterling, *Numerical Recipes in C. The Art of Scientific Programming*. New York: Cambridge University Press (1992) 994pp.
17. E. J. Doedel, A. R. Champneys, T. F. Fairgrieve, Y. A. Kuznetsov, B. Sandstede and X. Wang, AUTO 97: Continuation and bifurcation software for ordinary differential equations. (1997). Available via anonymous ftp from `ftp://ftp.cs.concordia.ca/pub/doedel/auto`.